Geomechanics and Engineering, *Vol. 30, No. 4 (2022) 345-352*
https://doi.org/10.12989/gae.2022.30.4.345

Stiffness effect of testing machine indenter on energy evolution of rock under uniaxial compression

Yunliang Tan[1,2,3a], Qing Ma*[2], Cunwen Wang[3b] and Xuesheng Liu[1,2c]

[1]*State Key Laboratory of Mining Disaster Prevention and Control Co-founded by Shandong Province and the Ministry of Science and Technology, Qingdao 266590, China*
[2]*College of Energy and Mining Engineering, Shandong University of Science and Technology, Qingdao, 266590, China*
[3]*Shandong Energy Group, Jinan 250014, China*

(*Received April 19, 2021, Revised April 12, 2022, Accepted July 23, 2022*)

Abstract. When rock burst occurs, the damaged coal, rock and other fragments can be ejected to the roadway at a speed of up to 10 m/s. It is extremely harmful to personnel and mining equipment, and seriously affects the mining activities. In order to study the energy evolution characteristics, especially kinetic energy, in the process of rock mass failure, this paper first analyzes the energy changes of the rock in different stages under uniaxial compression. The formula of the kinetic energy of rock sample considering the energy from the indenter of the testing machine is obtained. Then, the uniaxial compression tests with different stiffness ratios of the indenter and rock sample are simulated by numerical simulation. The kinetic energy U_d, elastic strain energy U_e, friction energy U_f, total input energy U and surface energy U_θ of crack cracking are analyzed. The results show that: The stiffness ratio has influence on the peak strength, peak strain, U_d, U_e, U_θ, U_f and U of rock samples. The variation trends of strength, strain and energy with stiffness are different. And when the stiffness ratio increases to a certain value, if the stiffness of the indenter continues to increase, it will have no longer effect on the rock sample.

Keywords: kinetic energy; rock burst; stiffness; testing machine; uniaxial compression

1. Introduction

Rock burst is a phenomenon that the high strength coal and rock deformation energy is released in the mining activity, which causes strong rock vibration and extrusion in the corresponding mining space. It is one of the main dynamic disasters in coal mining (Tan *et al*. 2009, Fakhimi *et al*. 2016, Whyatt and Blake 2002, Du *et al*. 2020). When rock burst occurs, coal, rock blocks, fragments and particles of different sizes are often ejected or thrown into roadways. The speed of the broken blocks, fragments and particles sometimes even exceeds 10m/s. It is extremely harmful to personnel and equipment, and seriously affects the construction progress (Wang *et al*. 2019, Leveille *et al*. 2017, Bieniawski 1968, Qiu *et al*. 2022, Ma *et al*. 2020). Therefore, the study of energy, especially kinetic energy in the process of coal and rock mass failure, is of great significance to the construction of deep underground rock engineering.

For the calculation method of coal and rock kinetic energy in the process of rock burst, scholars have carried out extensive theoretical and laboratory research. Zuo *et al*. (2006) discussed the type of rock ejection velocity and its significance in the design of rock burst dangerous roadway support based on the physical process of rock burst and the manifestation of rock burst. The energy composition of the rock burst and the ejection velocity of the rock block induced by the uniaxial dynamic and static combined loading are calculated. Qin *et al*. (2011) discussed the high-speed ejection mechanism of the block in the rock burst problem, and analyzed the energy of the block after instability. It is obtained that the block velocity can reach 10 m/s, and it is concluded that the tensile strength of the rock mass also affects the magnitude of the block velocity. He *et al*. (2010) conducted theoretical and experimental studies on the ejection velocity of rock bursts in deep mining, and established a theoretical model of the ejection velocity during rock bursts. The ejection velocities of the three typical motion forms of rock blocks are calculated and compared with the experimental values obtained from the rock burst experiment. Su *et al*. (2016) carried out a series of researches on the kinetic energy in the process of rock burst, including discrete element simulation of rock burst ejection failure under excavation unloading and disturbance load, experimental research on hard rock burst ejection failure process, release mechanism of ejection kinetic energy of strain rock burst and quantitative prediction method, etc. The quantitative analysis method of kinetic energy of rock burst is obtained from numerical simulation and laboratory tests. The above research studies the energy evolution in the process of rock burst from different

*Corresponding author, Ph.D. Student
E-mail: qingma819@126.com
[a]Professor
E-mail: yunliangtan@163.com
[b]Professor
E-mail: wangcunwen@163.com
[c]Professor
E-mail: xuesheng1134@163.com

ISSN: 2005-307X (Print), 2092-6219 (Online)

perspectives. The kinetic energy release mechanism and its calculation method are obtained, which makes an important contribution to the prediction and prevention of rock burst.

In fact, when rock burst occurs, the kinetic energy in coal and rock mass includes not only the elastic strain energy contained in coal and rock mass itself, but also the energy released when the roof and floor rocks are damaged. At this time, the entire surrounding rock is equivalent to a large loading test machine (Xu and Cai 2017, Salamon 1970, 1984, Hudson *et al*. 1972, Vardar *et al*. 2017, Que *et al*. 2022). When multiple coal seams are mined, a large number of coal pillars are left. The roof and floor types upper or under coal pillars are different. When other conditions are the same, surrounding rocks of different properties can be regarded as test machines with different stiffness for loading (Xu and Cai 2017, Salamon 1970, 1984, Hudson *et al*. 1972, Vardar *et al*. 2017). But the existing test equipment is mostly rigid test machine. Due to the fixed loading rigidity of the testing machine, which does not match the actual loading conditions of the site project, the experimental results obtained are quite different from the actual site project. Different stiffness directly affects the kinetic energy when coal and rock mass are destroyed (Xu and Cai 2017, Wang and Kaunda 2019). Depending on the stiffness of the roof and floor rock, how much energy is provided for the failure and instability of coal and rock masses, and what is the kinetic energy provided by the remaining energy transformation. Although great progress has been made in studying the energy mechanisms of rock failure, the details of kinetic energy of the rock mass, the surface energy of crack cracking and the frictional energy consumption when the indenter has different stiffness has not been fully explained.

This article first analyzes the energy in the process of rock deformation and failure during uniaxial compression. Then, the numerical simulation method is used to analyze the changes of various energy during the failure process of the rock sample under uniaxial compression. And the proportion of all kinds of energy in the total energy under different roof and floor stiffness environment is obtained.

2. Engineering background

Coal pillars can be defined as coal bodies that are mined out on two or more sides in underground mining (Sun *et al*. 2017, Kias and Ozbay 2013, Bertuzzi *et al*. 2016, Esterhuizen *et al*. 2011, Guy *et al*. 2017, Ma *et al*. 2021). In various coal mining methods, a large number of coal pillars are required to be used for controlling ground subsidence, supporting roofs, protecting roadways, isolating water and sand and other possible disasters. It mainly includes ground buildings protective coal pillar, isolated coal pillar, waterproof coal pillar and roadway coal pillar, etc. (Sun *et al*. 2017, Kias and Ozbay 2013, Bertuzzi *et al*. 2016, Esterhuizen *et al*. 2011). After coal mining, the remaining coal pillars are prone to local stress concentration. As time goes by, the coal pillars will weather, creep, and rupture naturally, which may cause coal pillar-stratum linkage instability and damage (Yu *et al*. 2014, Zhao 2018). There are more coal pillars left when mining in multiple coal seams, and more disasters will be generated accordingly. In recent years, many old mines in China, such as Datong, Beijing, Yanzhou, Xinwen, Jining coal field, etc., have lost stability due to a large number of residual coal pillars during early mining, causing sudden collapse of the upper goaf rock strata. It has strong dynamic pressure impact on the mining of the lower coal seam, resulting in severe deformation and damage of the support and mining roadway (Yu *et al*. 2014, Zhao 2018). The roof and floor lithologies are different when pillars are left in different coal seams in multi coal seam mining. When other conditions are the same, surrounding rocks of different lithologies can be regarded as loading by the testing machine with different stiffness (Xu and Cai 2017, Salamon 1970, 1984, Hudson *et al*. 1972). Since Cook *et al*. (1965) successfully developed a rigid testing machine in 1965 and obtained the load-displacement curve of the rock for the first time, the concept of the effect of the stiffness of the loading body on the test results has been widely accepted. Experimental research is one of the most basic methods to reveal the disaster mechanism and energy evolution law of rock burst (Xu and Cai 2017, Wang and Kaunda 2019, Su *et al*. 2017). The energy evolution characteristics of rock samples in uniaxial compression process with different stiffness ratios of indenter and rock sample will be studied by numerical simulation tests.

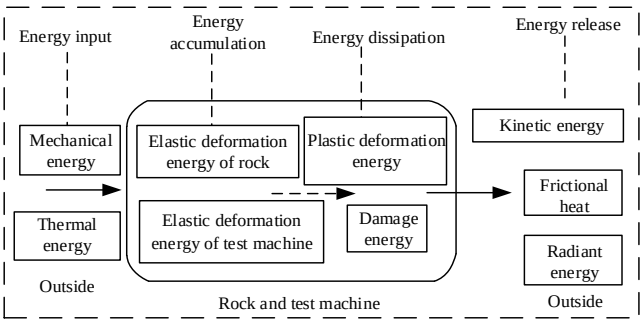

Fig. 1 Energy change during rock deformation and failure (Zhang *et al*. 2013)

3. Energy change during rock uniaxial compression test

According to the law of thermodynamics, the destruction of any substance is closely related to its energy change, and essentially occurs under the drive of energy (Solecki and Conant 2003, Xie *et al*. 2005, Maruvanchery *et al*. 2019, Wang and Kaunda 2019). Therefore, studying the occurrence process of rock burst from the energy point of view is a reliable way to reveal its true occurrence mechanism. The whole process of rock deformation and destruction will be accompanied by the accumulation, dissipation and release of energy. External energy input part of the energy accumulation is mainly the elastic strain energy accumulated in the coal and rock body, which is released when it is broken. The other part is transformed into energy dissipation such as rupture surface energy, electromagnetic radiation, infrared radiation, and acoustic

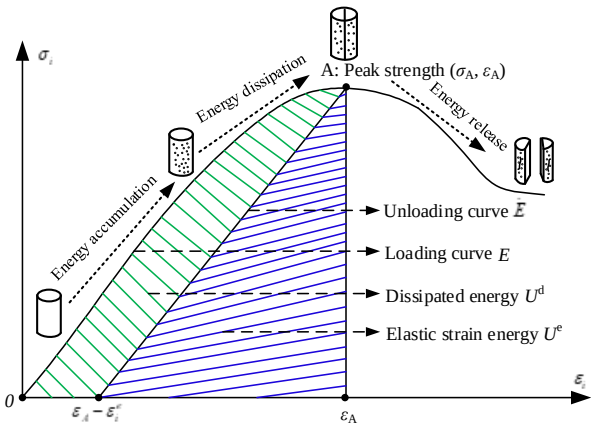

Fig. 2 The relationship between dissipated energy and releasable strain energy during rock uniaxial compression (Xie *et al*. 2005, Zhang *et al*. 2013)

emission. When the rock is damaged, the energy released mainly includes acoustic wave energy, radiation energy, kinetic energy, frictional heat energy, etc, as shown in Fig. 1 (Zhang *et al*. 2013).

The following is a detailed analysis of the energy change of the rock during uniaxial compression as an example. The relationship between dissipated energy and releasable strain energy during rock uniaxial compression is shown in Fig. 2.

The energy changes of rock in different stages of uniaxial compression can be divided into the following processes. (a) Fracture compaction stage: In this stage, the external force does work on the rock, and the internal fissures are continuously compacted under the action of the external force. (b) Elastic stage: At this stage, the rock can be regarded as an elastic body, which can return to the initial state when unloading. The work done by the external force will be converted into the elastic strain energy U_e of the rock, the elastic strain energy U_s of the testing machine and the energy U_r consumed by the various damping of the testing machine. At this stage

$$U = U_s + U_e + U_r \tag{1}$$

Generally speaking, the energy U_r consumed by the various damping of the testing machine is small, so it can be ignored. (c) Crack initiation and cracking stage: At this time, under the action of external force, new micro cracks begin to sprout and expand. At this stage, part of the external input energy is converted into the elastic strain energy of the rock and the testing machine, and the other part is dissipated by the nonlinear mechanism inside the rock. The energy dissipated mainly includes plastic potential energy U_p and damage potential U_d. The plastic potential energy U_p is the thermal energy T, and the damage potential energy U_c is mainly the surface energy U_θ of cracks cracking. At this stage

$$U = U_s + U_e + T + U_\theta \tag{2}$$

(d) The crack propagates rapidly to the failure stage: Affected by the external force, the deformation continues. When the peak point of the rock is reached, a large number of micro-cracks are generated, expanded, merged, and finally penetrated to form a macroscopic main crack. At this stage, it mainly includes the surface energy U_θ of cracks cracking, the elastic strain energy U_e of the rock sample, and the stored elastic strain energy U_s of the indenter of the testing machine. But at the moment of failure of the rock sample, the stored elastic strain energy is largely converted into the kinetic energy U_d when the rock is broken and ejected, and friction between the fragments and between the rock and the indenter of the testing machine will generate frictional heat U_f when the rock is ejected, And energy U_w such as sonic energy and radiation energy. At this stage

$$U_e = U_d + U_f + U_w \tag{3}$$

$$U = U_s + U_d + U_f + U_w + U_\theta \tag{4}$$

The energy calculation formula of the rock is as follows (Zhang *et al*. 2013, Solecki and Conant 2003, Xie *et al*. 2005, Wang and Kaunda 2019)

$$U = \int_0^{\varepsilon_1} \sigma_1 d\varepsilon_1 + \int_0^{\varepsilon_2} \sigma_2 d\varepsilon_2 + \int_0^{\varepsilon_3} \sigma_3 d\varepsilon_3 \tag{5}$$

$$U^e = \frac{1}{2\bar{E}}[\sigma_1^2 + \sigma_2^2 + \sigma_3^2 - 2\bar{\nu}(\sigma_1\sigma_2 + \sigma_2\sigma_3 + \sigma_1\sigma_3)] \tag{6}$$

Where: $\bar{E}$ and $\bar{\nu}$ are the average values of unloading elastic modulus and Poisson's ratio, respectively.

Eq. (6) is the calculation formula that can release the elastic strain energy under triaxial compression. When the rock undergoes uniaxial compression, the Eq. (6) becomes

$$U^e = \frac{\sigma_1^2}{2\bar{E}} \tag{7}$$

According to the research of Chen *et al*. (2010), the calculation formula of the surface energy U_θ of crack cracking and frictional energy U_f can be obtained as follows (Chen *et al*. 2010)

$$U_\theta = \frac{(1-\nu^2)\pi h\sigma^2 a\cos^2\alpha\sin^2\alpha}{4E} \tag{8}$$

$$U_f = \frac{ah\sigma^2\tan\varphi\cos^2\alpha}{E\sin\alpha} \tag{9}$$

Where: ν is the Poisson's ratio, h is the height of the specimen, a is the bottom area of the specimen, E is the elastic modulus of the specimen, α is the fracture angle of the rock, φ is the internal friction angle of the rock, $\alpha = \frac{\pi}{4} + \frac{\varphi}{2}$.

4. Numerical calculation model

Fig. 3(a) is an indoor rock uniaxial compression experiment. In order to accurately simulate the indoor uniaxial compression test, a uniaxial loading finite difference model is established in FLAC3D, as shown in Fig. 3(b). The diameter of the rock sample is 50 mm and the height is 100 mm. Both the rock sample and the indenter adopt column elements. The rock sample is divided into 160,000 elements, and the indenter is divided into 2,560 elements. The indenter is set as a linear elastic body, and the rock sample adopts a strain softening model (Hoek 2000) (The stress-strain curve is shown in Fig. 4). In order to analyze the energy evolution characteristics of the rock sample and the indenter when the indenter has different

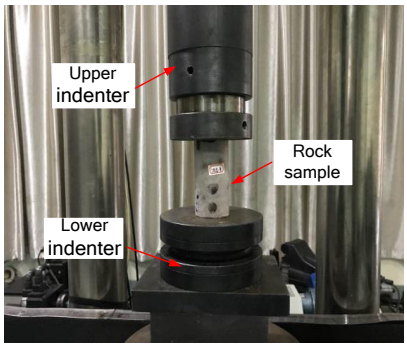

(a) Uniaxial compression photos of rock samples during indoor test

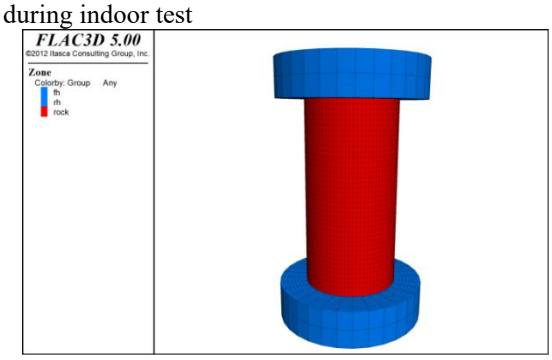

(b) Numerical calculation model and meshing

Fig. 3 Indoor uniaxial compression test sample loading diagram, calculation model, and grid division

stiffnesses and the stiffness ratio of the indenter to the rock sample is assumed to be $\alpha = E_h/E_r$. Where E_h and E_r are the elastic modulus of the indenter and the rock sample, respectively. Under the condition that other basic parameters of the indenter of the testing machine remain unchanged, the relationship between the failure of rock samples and the stiffness of the indenter can be obtained by changing the elastic modulus of the indenter. The material parameters used for the indenter and the rock sample are shown in Table 1.

5. Energy analysis during the test

Since this article focuses on the impact of indenter stiffness on the energy evolution during the failure process of rock samples, detailed analysis of the uniaxial and triaxial compressive stress-strain test curves of rock samples with different stiffness will not be carried out. Only the stress-strain curves of rock samples under uniaxial compression and triaxial compression when the stiffness ratio is 1 are listed, as shown in Fig. 5. Table 2 shows the mechanical parameters of rock samples with different stiffness ratios. It can be seen from Fig. 5 and Table 2 that

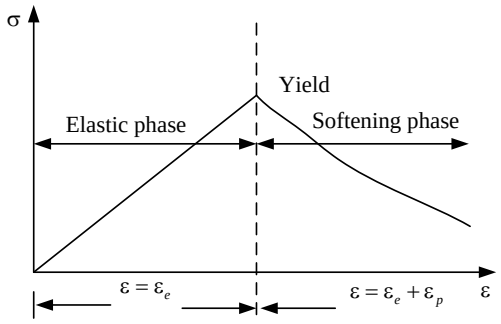

Fig. 4 Stress-strain curve (Hoek 2000, Saticia *et al*. 2020, Gkikas *et al*. 2020, Huismans 2002)

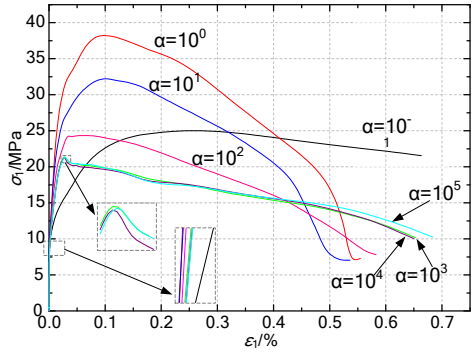

(a) Uniaxial compression stress-strain curve

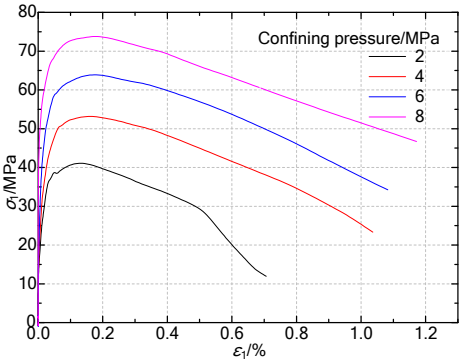

(b) Triaxial compression stress-strain curve when stiffness ratio α=1

Fig. 5 The uniaxial compressive stress-strain curve of rock samples with different stiffness ratios and the triaxial compressive stress-strain curve when stiffness ratio α=1

as the stiffness ratio increases, the peak strength of the rock sample in uniaxial compression first increases and then decreases. When the stiffness ratio α increases from 0.1 to 1, the uniaxial compressive strength increases from 25.0 MPa to 38.2 MPa, an increase of 52.8%. As the stiffness ratio α increases to 1000, the uniaxial compressive strength decreases from 38.2 MPa to 21.4 MPa, which is a 44.0% reduction. When the stiffness ratio α is increased to 10,000

Table 1 Material parameter table for numerical calculation of indenter and rock sample

Material	Elastic modulus/GPa	Poission's ratio μ	Cohesion/MPa	Internal friction angle /°	Tensile strength /MPa
Indenter	0.15/1.5/15/150/1500/15000/150000	0.2	/	/	/
Rock sample	1.5	0.272	2.5	40	0.5

Table 2 Mechanical parameters of rock samples with different stiffness ratios

Stiffness ratios	Cohesion /MPa	Internal friction angle /°	Peak strength /MPa	Peak strain/%
10^{-1}	8.1	54.59	25.0	0.24
10^{0}	12	56.16	38.2	0.09
10^{1}	8.8	57.41	32.2	0.11
10^{2}	7	54.43	24.3	0.06
10^{3}	5.2	54.87	21.4	0.03
10^{4}	4.5	55.86	21.3	0.03

and 100,000, the stress-strain and peak strength of the rock sample in uniaxial compression no longer change significantly. That is, when the indenter stiffness of the testing machine is large enough relative to the sample, the indenter stiffness continues to increase and will no longer affect the deformation and failure of the sample. The peak strain in uniaxial compression shows a decreasing trend as the stiffness ratio increases. When the stiffness ratio α is increased from 0.1 to 10000, the peak strain decreases from 0.24% to 0.03%, which is a decrease of 87.5%.

When the indenter and the rock sample have different stiffness ratios, the kinetic energy U_d, elastic strain energy U_e, frictional energy U_f, total input energy U and the surface energy U_θ of crack cracking with strain during uniaxial compression of the rock sample are shown in Fig. 6. It can be seen from Fig. 6 that the kinetic energy U_d and frictional energy U_f of the rock sample show a decreasing trend with the increase of the stiffness ratio. When the rock sample is broken, the energy is released at the moment, the value of kinetic energy and frictional energy consumption is the largest. Then the kinetic energy gradually decreases as the strain increases. At the same strain, as the stiffness ratio increases, the total input energy U increases first and then decreases as the stiffness ratio increases. At the same stiffness ratio, the total input energy shows an increasing

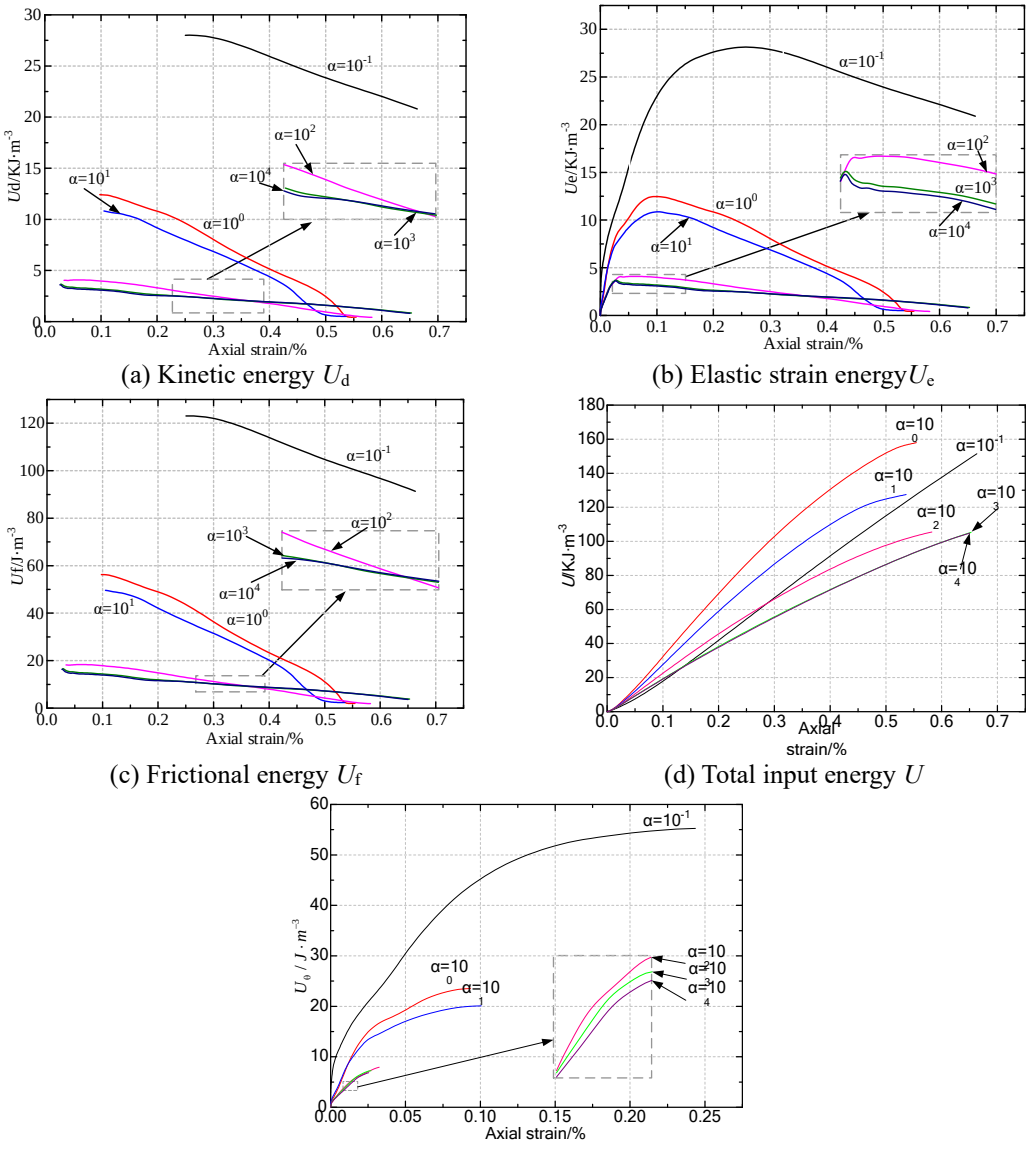

(a) Kinetic energy U_d

(b) Elastic strain energyU_e

(c) Frictional energy U_f

(d) Total input energy U

(e) Surface energy of cracks cracking U_θ

Fig. 6 Variations of various energy with strain at different stiffness ratios

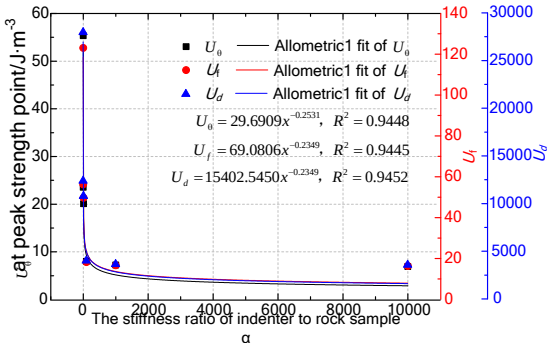

Fig. 7 The change of energy at peak strength at different stiffness ratios

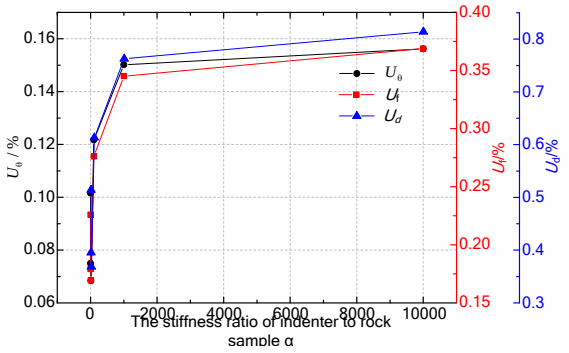

Fig. 8 The proportion of various energies when the rock sample fails at different stiffness ratios

trend with the increase of strain. The surface energy of crack cracking shows a decreasing trend as the stiffness ratio increases at the same strain. At the same stiffness ratio, it shows an increasing trend with the increase of strain.

Fig. 7 shows the U_e, U_f, and U_d at the peak strength at different stiffness ratios. The three of them all show a non-linear decreasing trend with the increase of stiffness ratio. Fitting with Allometric function can well represent its trend of change. The change trend of the elastic strain energy U_e at the peak strength as the stiffness ratio increases can be expressed by the function $U_e = 29.6909x^{-0.2531}$, where R^2=0.9448. The fitting function of the trend of frictional energy consumption U_f with increasing stiffness ratio is $U_f = 69.0806x^{-0.2349}$, where R^2=0.9445. The fitting function of the trend of kinetic energy U_d with increasing stiffness ratio is, where R^2=0.9452.

In order to better analyze the effect of stiffness ratio on the energy evolution of rock samples under uniaxial compression, the surface energy of cracks cracking U_θ, frictional energy U_f and kinetic energy U_d proportions of rock sample cracks at different stiffness ratios are drawn, as shown in Fig. 8. The proportion of the three is increasing with the increase of the stiffness ratio. When the stiffness ratio is the same, the kinetic energy U_d accounts for the largest proportion, the frictional energy consumption U_f takes the second place, and the surface energy of cracks cracking U_θ accounts for the smallest proportion.

6. Conclusions

With the stiffness ratio increases, the peak strength of the rock sample in uniaxial compression increases first and then decreases. When the stiffness ratio increases to 10000 and 100000, the stress-strain curve and peak strength of rock samples do not change significantly. The peak strain shows a decreasing trend as the stiffness ratio increases. When the stiffness ratio is increased from 0.1 to 10000, the peak strain decreases from 0.24% to 0.03%, which is a decrease of 87.5%.

The kinetic energy U_d and frictional energy U_f of the rock sample show a decreasing trend with the increase of stiffness ratio. The peak value of elastic strain energy U_e shows a decreasing trend as the stiffness ratio increases. The total input energy U increases first and then decreases as the stiffness ratio increases. The surface energy U_θ of crack cracking shows a decreasing trend with the increase of the stiffness ratio.

The elastic strain energy U_e, frictional energy U_f and kinetic energy U_d at the peak strength all show a nonlinear decreasing trend with the increase of stiffness ratio. The ratio of surface energy U_θ, frictional energy U_f and kinetic energy U_d to the total energy of crack cracking increases with the increase of stiffness ratio. When the stiffness ratio is the same, the kinetic energy U_d accounts for the largest proportion, the frictional energy consumption U_f takes the second place, and the cracking surface energy U_θ accounts for the smallest proportion.

The effect of the stiffness on the test results should be considered when testing the mechanical properties of the rock sample. Since the testing machine cannot be an ideal rigid body, the work done by the external load is not completely converted into the energy absorbed by the deformation and failure of the rock sample. But when the stiffness of the indenter is large enough relative to the stiffness of the rock sample, the stiffness of the indenter will have no longer effect on the rock sample.

However, there are still many issues needs to be further studied: (1) the next step should be combined with indoor experiments to conduct research to better guide engineering practice; (2) the influences of, loading rate, rock sample size, rock heterogeneity and so on; (3) when the stiffness of the upper and lower indenters is different, what will happen to the rock sample.

Acknowledgments

This study was financially supported by Major Scientific and Technological Innovation Project of Shandong Provincial Key Research Development Program (Grant No. 2019SDZY02) and National Natural Science Foundation of China (Grant No. 52074168, No. 51874190).

References

Bertuzzi, R., Douglas, K. and Mostyn, G. (2016), "An approach to model the strength of coal pillars", *Int. J. Rock Mech. Min.*, **89**, 165-175. https://doi.org/10.1016/j.ijrmms.2016.09.003.

Bieniawski, Z.T. (1968), "Note on in situ testing of the strength of coal pillars", *J. South. Afr. Inst. Min. Metal*., **68**(10), 1-12.

Chen, X.G. and Zhang, Q.Y. (2010), "Research on the energy dissipation and release in the process of rock shear failure", *J. Min. Saf. Eng*., **27**(2), 179-184. https://doi.org/10.3969/j.issn.1673-3363.2010.02.008.

Cook, N. (1965), "The failure of rock", *Int. J. Rock Mech. Min. Sci*., **2**(4), 389-403. https://doi.org/10.1016/0148-9062(65)90004-5.

Du, F. and Wang, K. (2020), "The mechanism of rockburst-outburst coupling disaster considering the coal-rock combination: an experiment study", *Geomech. Eng*., **22**(3), 255-264. https://doi.org/10.12989/gae.2020.22.3.000.

Esterhuizen, G.S., Dolinar, D.R., Ellenberger, J.L. and Prosser, L.J. (2011), "Pillar and roof span design guidelines for underground stone mines", National Institute for Occupational Safety and Health, Pittsburgh, PA.

Fakhimi, A., Hosseini, O. and Theodore, R. (2016), "Physical and numerical study of strain burst of mine pillars", *Comput. Geotech*., **74**, 36-44. http://10.1016/j.compgeo.2015.12.018.

Gkikas, V.I. and Nomikos, P.P. (2020), "Primary support design for sequentially excavated tunnel junctions in strain-softening hoek-brown rock mass", *Geotech. Geolo. Eng*., **39**(3), 1997-2018. https://doi.org/10.1007/s10706-020-01602-0.

Guy, R., Kent, M. and Russell, F. (2017), "An assessment of coal pillar system stability criteria based on a mechanistic evaluation of the interaction between coal pillars and the overburden", *Int. J. Min. Sci. Technol*., **27**(1), 11-17. https://doi.org/10.1016/j.ijmst.2016.09.031.

He, M.C. and Miao, J.L. (2010), "Rock burst process of limestone and its acoustic emission characteristics under true-triaxial unloading conditions", *Int. J. Rock Mech. Min. Sci*., **47**(2), 286-298. http://10.1016/j.ijrmms.2009.09.003.

Hoek, E. (2007), "Rock mechanics", *Institution of Mining and Metallurgy*, London.

Hudson, J.A., Crouch, S.L. and Fairhurst, C. (1972), "Soft, stiff and servo-controlled testing machines: A review with reference to rock failure", *Eng. Geol*., **6**(3), 155-189. https://doi.org/10.1016/0013-7952(72)90001-4.

Huismans, R.S. and Beaumont, C. (2002), "Asymmetric lithospheric extension: the role of frictional plastic strain softening inferred from numerical experiments", *Geology*, **30**(3), 211-214. https://doi.org/10.1130/0091-7613(2002)0302.0.CO;2.

Kias, E. and Ozbay, U. (2013), "Modeling unstable failure of coal pillars in underground mining using the discrete element method", *47th US Rock Mech Symposium*.

Leveille, P., Sepehri, M. and Apel, D.B. (2017), "Rockbursting potential of Kimberlite: a case study of diavik diamond mine", *Rock Mech. Rock Eng*., **50**(3), 1-9. https://doi.org/10.1007/s00603-017-1294-z.

Ma, Q., Tan, Y.L., Liu, X.S., Gu, Q.H. and Li, X.B. (2020), "Effect of coal thicknesses on energy evolution characteristics of roof rock-coal-floor rock sandwich composite structure and its damage constitutive model", *Compos. Part B-Eng*., **198**, 108086. https://doi.org/10.1016/j.compositesb.2020.108086.

Ma, Q., Tan, Y.L., Liu, X.S., Zhao, Z.H. and Fan, D.Y. (2021), "Mechanical and energy characteristics of coal-rock composite sample with different height ratios: a numerical study based on particle flow code", *Environ. Earth Sci*., **80**(8), 1-14. https://doi.org/10.1007/s12665-021-09453-5.

Maruvanchery, V. and Kim, E. (2019), "Effects of water on rock fracture properties: Studies of mode i fracture toughness, crack propagation velocity, and consumed energy in calcite-cemented sandstone", *Geomech. Eng*., **17**(1), 57-67. https://doi.org/10.12989/gae.2019.17.1.057.

Qin, J.F. and Zhuo, J.S. (2011), "A discussion on rock velocity in rockburst", *Rock Soil Mech*., **32**(5), 1365-1368. https://doi.org/10.1631/jzus.B1000185.

Qiu, L., Zhu, Y., Song, D., He, X., Wang, W., Liu, Y., ... & Liu, Q. (2022), "Study on the nonlinear characteristics of EMR and AE during coal splitting tests", *Miner*., **12**(2), 108. https://doi.org/10.3390/min12020108.

Que, Y., Chen, X., Chen, Y., Jiang, Z., Qiu, Y. and Easa, S. (2022), "Stability analysis of double V-shaped gully embankment: dimension-reduced calculation method", *Can. J. Civil Eng*., **49**(1), 52-63. https://doi.org/10.1139/cjce-2019-0783.

Salamon, M.D.G. (1970), "Stability, instability and design of pillar workings", *Int. J. Rock Mech. Min. Sci*., **7**(6), 613-631. https://doi.org/10.1016/0148-9062(70)90022-7.

Salamon, M.D.G. (1984), "Energy considerations in rock mechanics: fundamental results", *J. South African Inst. Min. Metal*., **84**(8), 233-46. https://doi.org/10.1016/0022-3115(84)90073-4.

Saticia, O. and Tamer, T. (2020), "Assessment of damage zone thickness and wall convergence for tunnels excavated in strain-softening rock masses", *Tunnel. Underg. Space Technol*., **108**, 103722. https://doi.org/10.1016/j.tust.2020.103722.

Solecki, R. and Conant, R.J. (2003), *Advanced Mechanics of Materials*, University Press London, Oxford.

Su, G,S., Jiang, J.Q., Zhai, S.B. and Zhang, G.L. (2017), "Influence of tunnel axis stress on strainburst: an experimental study", *Rock Mech. Rock Eng*., **50**(6), 1551-1567. https://doi.org/10.1007/s00603-017-1181-7.

Sun, W., Zhang, Q., Luan, Y. and Zhang, X.P. (2018), "A study of surface subsidence and coal pillar safety for strip mining in a deep mine", *Environ. Earth Sci*., **77**(17), 627. https://doi.org/10.1007/s12665-018-7810-y.

Tan, Y.L., Sun, C.J. and Zhang, Z.Y., (2009), "2D-ball simulations on stiffness influences for coal bump", *J. Coal Sci. Eng. (China)*, **15**(2), 161-165.

Vardar, O., Tahmasebinia, F., Zhang, C., Canbulat, I. and Saydam, S. (2017), "A review of uncontrolled pillar failures", *Procedia Eng*., **191**, 631-637. https://doi.org/10.1016/j.proeng.2017.05.227.

Wang, F. and Kaunda, R. (2019), "Assessment of rockburst hazard by quantifying the consequence with plastic strain work and released energy in numerical models", *Int. J. Min. Sci. Tech*., **29**(1), 89-93. https://doi.org/10.1016/j.ijmst.2018.11.023.

Wang, G.F., Gong, S.Y., Dou, L.M., Cai, W., Yuan, X.Y. and Fan, C.J. (2019). "Rockburst mechanism and control in coal seam with both syncline and hard strata", *Saf. Sci*., **115**, 320-328. https://doi.org/10.1016/j.ssci.2019.02.020.

Whyatt, J.W. and Blake, T.W. (2002), "60 years of rockbursting in the Coeur D'alene district of northern Idaho", Lessons Learned and Remaining Issues, USA.

Xie, H.P., Peng, R.D., Ju, Y. and Zhou, H.W. (2005), "Energy analysis of rock failure", *Chin. J. Rock Mech. Eng*., **24**(15), 2603-2608. https://doi.org/10.3321/j.issn:1000-6915.2005.15.001.

Xu, Y.H. and Cai, M. (2017), "Influence of loading system stiffness on post-peak stress-strain curve of stable rock failures", *Rock Mech. Rock Eng*., **50**, 2255-2275. https://doi.org/10.1007/s00603-017-1231-1.

Yu, B., Liu, C.Y. and Liu, J.R. (2014), "Mechanism and control technology of pressure occurrence in roadway with extra thickness and mechanized caving coal seam in Datong Mining Area", *Chin. J. Rock Mech. Eng*., **33**(9), 1863-1872. https://doi.org/10.13722/j.cnki.jrme.2014.09.017.

Zhang, Z.Z. (2013), "Energy evolution mechanism during rock deformation and failure", Ph.D. Dissertation, China University of Mining and Technology, Xuzhou.

Zhao, J. (2018), "Study on evolution law of overburden structure and strata pressure control in multi seam mining", Ph.D. Dissertation, Shandong University of Science and Technology, Xuzhou.

Zuo, Y.J., Li, X.B., Zhang, Y.T. and Wang, W.H. (2006), "Calculation of ejection velocity of rock in rockburst caused by

static-dynamic coupling loading", *J. Cent. South Univ*., **37**(4), 191-195. https://doi.org/10.1016/S1005-8885(07)60042-9.

CC